Discrimination of textures with spatial correlations and multiple gray levels: supplemental document

1. Specification and construction of textures

The present approach to parameterizing and constructing maximum-entropy textures with multiple gray levels generalizes the method of [1] for black-and-white textures used in previous studies[2-6]. This extension proceeds in two stages. First, in the black-and-white case, each configuration of checks (e.g., two horizontally-adjacent checks) corresponds to a single type of correlation, but when there are multiple gray levels, each configuration corresponds to a family of correlations. Second, in the black-and-white case, each correlation is specified by a scalar, but when there are G gray levels (here, $G=3$ to $G=11$), each kind of correlation is specified by a set of $G-1$ independent variables – so that for $G>2$, this specification is a vector, rather than a scalar. These extensions, presented here in detail, are also outlined in Appendix A of [1].

1.1 Families of correlations

The starting point is a specification of the probabilities of each way of coloring a 2×2 block of checks. We denote each such probability by $p\begin{pmatrix} A_1 & A_2 \\ A_3 & A_4 \end{pmatrix}$, where each A_k denotes the gray level of a check, which we designate as an integer from 0 to $G-1$ (0 indicates black, $G-1$ indicates white). Since there are G choices for coloring each check, there are G^4 ways of coloring a 2×2 block.

The basic hurdle is that these G^4 block probabilities are not independent, and the number of constraints between them increases rapidly with G. An obvious constraint is that, since they are an exhaustive list of probabilities, they must sum to 1. But other constraints arise because these block probabilities must be consistent with a homogeneous texture. For example, the two ways of computing the probability of horizontal (1×2) blocks must lead to consistent results: one could focus on the upper checks A_1 and A_2 and sum ("marginalize") over the lower checks A_3 and A_4, or one could focus on the lower checks A_3 and A_4 and sum over the upper two checks A_1 and A_2. Dependencies among the block probabilities arise because these two computations must produce the same results. Further constraints arise from consideration of the probabilities of other configurations of checks: singletons and 2×1 blocks. We note that we are concerned here with "algebraic" dependencies, i.e., dependencies that determine one block probability from another and therefore reduce the number of independent parameters. (We are not concerned with dependencies that merely limit the range of one or more parameters, but do not change the number of degrees of freedom).

To obtain a new set of coordinates that untangles these dependencies, we use the procedure described in Appendix A of [1]. The new coordinates, denoted $\varphi\begin{pmatrix} s_1 & s_2 \\ s_3 & s_4 \end{pmatrix}$, are the discrete Fourier transforms of the block probabilities, where the transform is computed with respect to the gray level value in each check.

$$\varphi\begin{pmatrix} s_1 & s_2 \\ s_3 & s_4 \end{pmatrix} = \sum_{A_1=0}^{G-1}\sum_{A_2=0}^{G-1}\sum_{A_3=0}^{G-1}\sum_{A_4=0}^{G-1} p\begin{pmatrix} A_1 & A_2 \\ A_3 & A_4 \end{pmatrix} e^{-\left(\frac{2\pi i}{G}\right)\left(A_1 s_1 + A_2 s_2 + A_3 s_3 + A_4 s_4\right)}. \tag{S1}$$

Since this is a discrete transform, the Fourier transform variables s_k are also integers from 0 to $G-1$. The original block probabilities $p\begin{pmatrix} A_1 & A_2 \\ A_3 & A_4 \end{pmatrix}$ can be obtained from the new coordinates $\varphi\begin{pmatrix} s_1 & s_2 \\ s_3 & s_4 \end{pmatrix}$ by standard inversion of the discrete Fourier transform:

$$p\begin{pmatrix} A_1 & A_2 \\ A_3 & A_4 \end{pmatrix} = \frac{1}{G^4}\sum_{s_1=0}^{G-1}\sum_{s_2=0}^{G-1}\sum_{s_3=0}^{G-1}\sum_{s_4=0}^{G-1} \varphi\begin{pmatrix} s_1 & s_2 \\ s_3 & s_4 \end{pmatrix} e^{\left(\frac{2\pi i}{G}\right)\left(A_1 s_1 + A_2 s_2 + A_3 s_3 + A_4 s_4\right)}. \tag{S2}$$

In an analogous fashion, Fourier transform coordinates can be defined for any set of checks, including subsets of the 2×2 neighborhood. For example, the Fourier transform coordinates for the checks in the upper 1×2 block are defined by

$$\varphi\begin{pmatrix} s_1 & s_2 \\ & \end{pmatrix} = \sum_{A_1=0}^{G-1}\sum_{A_2=0}^{G-1} p\begin{pmatrix} A_1 & A_2 \\ & \end{pmatrix} e^{-\left(\frac{2\pi i}{G}\right)\left(A_1 s_1 + A_2 s_2\right)}, \tag{S3}$$

where $p\begin{pmatrix} A_1 & A_2 \\ & \end{pmatrix}$ denotes the probability that the upper two checks of a 2×2 block contain A_1 and A_2, regardless of the contents of the two lower checks.

The Fourier transform coordinates allow for removal of the dependencies described above because ignoring a check corresponds to setting the corresponding Fourier coordinate to zero. This allows us to express the consistency conditions simply in terms of the Fourier transform coordinates for the 2×2 block.

Consider, for example, the consistency condition for 1×2 blocks. Computed from the upper two checks, this quantity, is determined by summing $p\begin{pmatrix} A_1 & A_2 \\ A_3 & A_4 \end{pmatrix}$ over A_3 and A_4:

$$p\begin{pmatrix} A_1 & A_2 \\ & \end{pmatrix} = \sum_{A_3=0}^{G-1}\sum_{A_4=0}^{G-1} p\begin{pmatrix} A_1 & A_2 \\ A_3 & A_4 \end{pmatrix}. \tag{S4}$$

Substituting this expression into eq. (S3) shows that

$$\begin{aligned} \varphi\begin{pmatrix} s_1 & s_2 \\ & \end{pmatrix} &= \sum_{A_1=0}^{G-1}\sum_{A_2=0}^{G-1} p\begin{pmatrix} A_1 & A_2 \\ & \end{pmatrix} e^{-\left(\frac{2\pi i}{G}\right)\left(A_1 s_1 + A_2 s_2\right)} \\ &= \sum_{A_1=0}^{G-1}\sum_{A_2=0}^{G-1}\left(\sum_{A_3=0}^{G-1}\sum_{A_4=0}^{G-1} p\begin{pmatrix} A_1 & A_2 \\ A_3 & A_4 \end{pmatrix}\right) e^{-\left(\frac{2\pi i}{G}\right)\left(A_1 s_1 + A_2 s_2\right)} = \varphi\begin{pmatrix} s_1 & s_2 \\ 0 & 0 \end{pmatrix} \end{aligned}. \tag{S5}$$

Similarly, the Fourier transform coordinates of the 1×2 blocks computed from the lower two checks are defined by

$$\varphi\begin{pmatrix} & \\ s_3 & s_4 \end{pmatrix} = \sum_{A_3=0}^{G-1}\sum_{A_4=0}^{G-1} p\begin{pmatrix} & \\ A_3 & A_4 \end{pmatrix} e^{-\left(\frac{2\pi i}{G}\right)(A_3 s_3 + A_4 s_4)}, \tag{S6}$$

and, via a similar calculation to eq. (S5), are given by

$$\varphi\begin{pmatrix} & \\ s_3 & s_4 \end{pmatrix} = \varphi\begin{pmatrix} 0 & 0 \\ s_3 & s_4 \end{pmatrix}. \tag{S7}$$

Since the Fourier transform coordinates determine the original coordinates (and vice-versa), the consistency condition

$$p\begin{pmatrix} A_1 & A_2 \\ & \end{pmatrix} = p\begin{pmatrix} & \\ A_1 & A_2 \end{pmatrix} \tag{S8}$$

is equivalent to

$$\varphi\begin{pmatrix} s_1 & s_2 \\ 0 & 0 \end{pmatrix} = \varphi\begin{pmatrix} 0 & 0 \\ s_1 & s_2 \end{pmatrix}. \tag{S9}$$

The other consistency conditions can be written in an analogous form. The condition that computing the 2×1 block probabilities from either the left or right columns of the 2×2 block gives the same result is expressed by

$$\varphi\begin{pmatrix} s_1 & 0 \\ s_3 & 0 \end{pmatrix} = \varphi\begin{pmatrix} 0 & s_1 \\ 0 & s_3 \end{pmatrix}. \tag{S10}$$

The condition that the single-check probabilities are equal in all four positions is equivalent to

$$\varphi\begin{pmatrix} s & 0 \\ 0 & 0 \end{pmatrix} = \varphi\begin{pmatrix} 0 & s \\ 0 & 0 \end{pmatrix} = \varphi\begin{pmatrix} 0 & 0 \\ s & 0 \end{pmatrix} = \varphi\begin{pmatrix} 0 & 0 \\ 0 & s \end{pmatrix}. \tag{S11}$$

Also, the condition that the block probabilities sum to 1 can be written

$$\varphi\begin{pmatrix} 0 & 0 \\ 0 & 0 \end{pmatrix} = 1. \tag{S12}$$

In sum, the consistency conditions (eqs. (S9), (S10), and (S11)) can expressed in terms of the Fourier transform coordinates as follows: any argument of $\varphi\begin{pmatrix} s_1 & s_2 \\ s_3 & s_4 \end{pmatrix}$ that is zero can be replaced by an empty space, and the value of $\varphi\begin{pmatrix} s_1 & s_2 \\ s_3 & s_4 \end{pmatrix}$ must be unchanged by translating the remaining values within the 2×2 neighborhood.

Thus, if a set of block probabilities is consistent with a texture, its Fourier transform coordinates can be specified by the following quantities, which we designate the "reduced Fourier coordinates" (Table 1 of the main text): $\varphi(s_1)$, equal to the common value of the four expressions in eq. (S11) for the $G-1$ nonzero values of s; $\varphi(s_1 \quad s_2)$, equal to the common value of the two expressions in eq. (S9) for each of the $(G-1)^2$ pairs of nonzero values of s_1 and s_2; $\varphi\begin{pmatrix} s_1 \\ s_3 \end{pmatrix}$, equal to the common value of the two expressions in eq.(S10) for each of the $(G-1)^2$ pairs of nonzero values of s_1 and s_3, as well as other Fourier transform quantities not involved in constraints (because the nonzero coordinates cannot be translated within the 2×2 neighborhood). These coordinates are $\varphi\begin{pmatrix} s_1 & \\ & s_4 \end{pmatrix}$, $\varphi\begin{pmatrix} & s_2 \\ s_3 & \end{pmatrix}$, $\varphi\begin{pmatrix} s_1 & s_2 \\ s_3 & \end{pmatrix}$, $\varphi\begin{pmatrix} s_1 & s_2 \\ & s_4 \end{pmatrix}$, $\varphi\begin{pmatrix} s_1 & \\ s_3 & s_4 \end{pmatrix}$, $\varphi\begin{pmatrix} & s_2 \\ s_3 & s_4 \end{pmatrix}$, and $\varphi\begin{pmatrix} s_1 & s_2 \\ s_3 & s_4 \end{pmatrix}$, defining two-check, three-check, and four-check correlations. In all of these cases, the arguments s_k must be nonzero. Conversely, specifying these quantities uniquely determines the block probabilities via Fourier inversion (eq. (S2)).

In the black-and-white case ($G=2$), the only possible nonzero value for each s_k is 1, so specifying the location of the nonzero arguments of φ is the same as specifying its arguments completely. Thus, the only first-order coordinate is $\varphi(1)$; the second-order coordinates are $\varphi\begin{pmatrix} 1 & 1 \end{pmatrix}$, $\varphi\begin{pmatrix} 1 \\ 1 \end{pmatrix}$, $\varphi\begin{pmatrix} 1 & \\ & 1 \end{pmatrix}$, and $\varphi\begin{pmatrix} & 1 \\ 1 & \end{pmatrix}$; the third-order coordinates are $\varphi\begin{pmatrix} 1 & 1 \\ 1 & \end{pmatrix}$, $\varphi\begin{pmatrix} 1 & 1 \\ & 1 \end{pmatrix}$, $\varphi\begin{pmatrix} 1 & \\ 1 & 1 \end{pmatrix}$, and $\varphi\begin{pmatrix} & 1 \\ 1 & 1 \end{pmatrix}$; and the one fourth-order coordinate is $\varphi\begin{pmatrix} 1 & 1 \\ 1 & 1 \end{pmatrix}$. As shown in Table 1 of the main text, the reduced Fourier coordinates correspond to the binary texture coordinates { γ, β_{-}, $\beta_{|}$, $\beta_{\backslash}$, $\beta_{/}$, $\theta_{\ulcorner}$, $\theta_{\urcorner}$, $\theta_{\llcorner}$, $\theta_{\lrcorner}$, α } used by [1].

For $G\geq 3$, each choice for the locations of nonzero arguments of φ is associated with a family of correlations, rather than just a single correlation as in the black-and-white case, because the arguments s_k of the reduced Fourier coordinates range independently from 1 to $G-1$. Thus, we can count the independent parameters needed to specify 2×2 block probabilities: there are $n_1 = G-1$ choices for the first-order coordinates $\varphi(s)$; $n_2 = 4(G-1)^2$ choices for the second-order coordinates $\varphi\begin{pmatrix} s_1 & s_2 \end{pmatrix}$, $\varphi\begin{pmatrix} s_1 \\ s_3 \end{pmatrix}$, $\varphi\begin{pmatrix} s_1 & \\ & s_4 \end{pmatrix}$, and $\varphi\begin{pmatrix} & s_2 \\ s_3 & \end{pmatrix}$; $n_3 = 4(G-1)^3$ choices for the third-order coordinates, $\varphi\begin{pmatrix} s_1 & s_2 \\ s_3 & \end{pmatrix}$, $\varphi\begin{pmatrix} s_1 & s_2 \\ & s_4 \end{pmatrix}$, $\varphi\begin{pmatrix} s_1 & \\ s_3 & s_4 \end{pmatrix}$,and $\varphi\begin{pmatrix} & s_2 \\ s_3 & s_4 \end{pmatrix}$; and $n_4 = (G-1)^4$ choices for the fourth-order coordinates $\varphi\begin{pmatrix} s_1 & s_2 \\ s_3 & s_4 \end{pmatrix}$. The total parameter count is

$$\begin{aligned} n_{tot}(G) &= n_1 + n_2 + n_3 + n_4 \\ &= (G-1) + 4(G-1)^2 + 4(G-1)^3 + (G-1)^4 \ . \\ &= G(G-1)(G^2+G-1) \end{aligned} \qquad \text{(S13)}$$

This parameter count is 10 for $G = 2$ and 66 for $G = 3$.

The Fourier transform coordinates have two convenient properties. First, the random texture (a texture where the gray level in each location is chosen independently, and equally likely to be any of the G possible values) is at the origin of the parameter space. That is, each of the $n_{tot}(G)$ Fourier coordinates is zero. This will be demonstrated below. Second, the Fourier coordinates are "calibrated:" that is, near the origin of the space, entropy, which corresponds to discriminability by an ideal observer, depends only on the Euclidean distance to the origin. This property can be demonstrated via the approach of Appendix B of [1].

1.2 Specifying individual correlations: barycentric coordinates

While the Fourier transform coordinates account for the dependencies between block probabilities, they cannot be chosen arbitrarily, since their inverse transforms – the original block probabilities -- must be all real and in the range $[0,1]$. That is, while we have solved the problem of dependencies between different orders of correlations, we still need to address dependencies within correlations of each family. This can be handled via a second transformation, to barycentric coordinates. To motivate this strategy, we examine the transformation between block probabilities and Fourier coordinates, eqs. (S1) and (S2), first for $G = 2$ and then for $G = 3$. The critical component is the exponential, $e^{\pm\left(\frac{2\pi i}{G}\right)(A_1 s_1 + A_2 s_2 + A_3 s_3 + A_4 s_4)}$. For $G = 2$, this exponential term is equal to $+1$ or -1, depending on whether $\sum_{k=1}^{4} s_k A_k$ is even or odd. Thus, eq. (S1) shows that the Fourier coordinates are guaranteed to be real, and eq. (S2) shows that any choice of real values for the Fourier coordinates will yield real values for the block probabilities. Moreover, since each of the block probabilities can be no greater than 1, eq. (S1) shows that the Fourier coordinates must lie in the range $[-1,+1]$. Recognizing that $\varphi\begin{pmatrix} 0 & 0 \\ 0 & 0 \end{pmatrix} = 1$ (eq. (S12)), eq. (S2) also shows that choosing any single Fourier coordinate φ within this range, and setting the others to zero, is guaranteed to yield block probabilities in the range $[0,1]$, as they will all be equal to $\frac{1}{16}(1 \pm \varphi)$, depending on whether $\sum_{k=1}^{4} s_k A_k$ is even or odd.

However, consideration of $G = 3$ shows that this simplicity is not generic, as the exponential term $e^{\pm\left(\frac{2\pi i}{G}\right)(A_1 s_1 + A_2 s_2 + A_3 s_3 + A_4 s_4)}$ need not be real. But as in the black-and-white case, it only depends on the remainder of $\sum_{k=1}^{4} s_k A_k$ $(\bmod G)$.

This dependence motivates grouping the terms of eq. (S1) according to the value of this remainder. We therefore define

$$\sigma_{\begin{pmatrix} s_1 & s_2 \\ s_3 & s_4 \end{pmatrix},h} = \sum_{A_1=0}^{G-1}\sum_{A_2=0}^{G-1}\sum_{A_3=0}^{G-1}\sum_{A_4=0}^{G-1} p\begin{pmatrix} A_1 & A_2 \\ A_3 & A_4 \end{pmatrix}\delta_{\bmod G}\left(A_1 s_1 + A_2 s_2 + A_3 s_3 + A_4 s_4 - h\right), \quad \text{(S14)}$$

where $\delta_{\bmod G}(z)$ is 1 if z is a multiple of G, and zero otherwise. That is, $\sigma_{\begin{pmatrix} s_1 & s_2 \\ s_3 & s_4 \end{pmatrix},h}$ is the total probability of all blocks for which $A_1 s_1 + A_2 s_2 + A_3 s_3 + A_4 s_4$ has a remainder $(\bmod G)$ of h. They are therefore all real and non-negative. They also determine the Fourier coordinates, because the defining equation for the Fourier coordinates (eq. (S1)) can be re-expressed by collecting common values of the exponential:

$$\varphi\begin{pmatrix} s_1 & s_2 \\ s_3 & s_4 \end{pmatrix} = \sum_{h=0}^{G-1} \sigma_{\begin{pmatrix} s_1 & s_2 \\ s_3 & s_4 \end{pmatrix},h} e^{-\frac{2\pi i}{G}h}. \quad \text{(S15)}$$

A consequence of eq.(S15) is that for the fully random texture, the coordinates φ are all zero – since for any $\begin{pmatrix} s_1 & s_2 \\ s_3 & s_4 \end{pmatrix}$, all of the nonzero values of $\sigma_{\begin{pmatrix} s_1 & s_2 \\ s_3 & s_4 \end{pmatrix},h}$ are equal, and the exponentials associated with these terms are equally-spaced unit vectors on the circle. However, the σ 's are a redundant parameterization, since if $\sum_{k=1}^{4} s_k A_k = h$ ($\bmod G$), then $\sum_{k=1}^{4} q s_k A_k = qh$ ($\bmod G$) as well. That is,

$$\sigma_{\begin{pmatrix} s_1 & s_2 \\ s_3 & s_4 \end{pmatrix},h} = \sigma_{\begin{pmatrix} qs_1 & qs_2 \\ qs_3 & qs_4 \end{pmatrix},qh}. \quad \text{(S16)}$$

Our final step is to remove this redundancy. This step is simplest when G is prime. (We do not discuss the modifications required when G is composite as they are only needed for specific choices of s_k that are not relevant to the stimuli used in this study – these are cases in which all the s_k have a common factor that also divides G). We remove this redundancy by focusing on the position m of the first nonzero value of the arguments of φ (that is, $s_m \neq 0$ but $s_1, \ldots, s_{m-1}$ are all 0), and showing that all of these φ 's are determined by the subset of $\sigma_{\begin{pmatrix} s_1 & s_2 \\ s_3 & s_4 \end{pmatrix}}$'s for which $s_m = 1$. This follows from the properties of modular arithmetic. When G is prime, every integer $r \in \{1, \ldots, G-1\}$, has a unique inverse $q \in \{1, \ldots, G-1\}$ for which $qr = 1$ ($\bmod G$), which we denote by $q = r^{-1}$. We now choose $q = s_m^{-1}$ in eq. (S15), and apply eq. (S16). It follows that

$$\varphi\begin{pmatrix} s_1 & s_2 \\ s_3 & s_4 \end{pmatrix} = \sum_{h=0}^{G-1} \sigma_{\begin{pmatrix} qs_1 & qs_2 \\ qs_3 & qs_4 \end{pmatrix},qh} e^{-\frac{2\pi i}{G}h}. \quad \text{(S17)}$$

As h ranges over all values from 0 to $G-1$ $(\bmod G)$, so does qh ,but in a different order. Substituting $v = qh$ (so $h = q^{-1}v = s_m v$),

$$\varphi\begin{pmatrix} s_1 & s_2 \\ s_3 & s_4 \end{pmatrix} = \sum_{v=0}^{G-1} \sigma_{\begin{pmatrix} qs_1 & qs_2 \\ qs_3 & qs_4 \end{pmatrix},v} e^{-\frac{2\pi i}{G} s_m v}, \tag{S18}$$

where m is the index of the first nonzero s_k. Since the first nonzero value of qs_k is qs_m, and $q = s_m^{-1}$, this expresses $\varphi\begin{pmatrix} s_1 & s_2 \\ s_3 & s_4 \end{pmatrix}$ as a Fourier transform of σ's for which the first nonzero term is 1. We call these σ's "monic."

Applying this analysis to each of the subsets of a 2×2 block yields a transformation from the reduced Fourier coordinates into the monic σ's. As eqs. (S17) or (S18) show, σ's and φ's are discrete Fourier transform pairs, so the monic σ's can be calculated directly from the φ's and vice-versa. Explicitly, the Fourier coordinates and the monic σ's are related by

$$\begin{gathered} \varphi\begin{pmatrix} s_1 & s_2 \\ s_3 & s_4 \end{pmatrix} = \sum_{v=0}^{G-1} \sigma_{\begin{pmatrix} 1 & s_1^{-1}s_2 \\ s_1^{-1}s_3 & s_1^{-1}s_4 \end{pmatrix},v} e^{-\frac{2\pi i}{G} s_1^{-1} v} \\ \text{and} \\ \sigma_{\begin{pmatrix} 1 & s_1^{-1}s_2 \\ s_1^{-1}s_3 & s_1^{-1}s_4 \end{pmatrix},v} = \sum_{v=0}^{G-1} \varphi\begin{pmatrix} s_1 & s_2 \\ s_3 & s_4 \end{pmatrix} e^{\frac{2\pi i}{G} s_1^{-1} v} \end{gathered}, \tag{S19}$$

with analogous relationships for reduced Fourier coordinates that operate on subsets of the 2×2 block.

Thus, specifying the monic σ's and the reduced Fourier coordinates φ are interchangeable, and we have seen above that the latter parameterizes the block probabilities that are consistent with a homogeneous texture.

The final step is to group together the G values $(\sigma_{S,0}, \sigma_{S,1}, \ldots, \sigma_{S,G-1})$ as a single vectorial quantity $\vec{\sigma}_{\begin{pmatrix} s_1 & s_2 \\ s_3 & s_4 \end{pmatrix}}$, and to give this vector a geometric interpretation. This step is independent of the size of the block or the parameters s_k that specify S. Because $\sigma_S(h)$ is the probability that the linear combination of gray levels specified by S has a remainder of $h \pmod{G}$, these quantities must sum to 1 and each must be ≥ 0. This means that $\vec{\sigma}_S$ corresponds to the intersection of a hyperplane (the constraint that the quantities sum to 1) and the sector of G-dimensional space in all coordinates are non-negative. For example, for $G = 3$, the three values $\vec{\sigma}_S = (\sigma_{S,0}, \sigma_{S,1}, \sigma_{S,2})$ are the coordinates of the points within an equilateral triangle whose vertices are at $(1,0,0)$, $(0,1,0)$, and $(0,0,1)$. For the generic G, $\vec{\sigma}_S$ corresponds to a regular simplex in dimension $G-1$, with its vertices at unit distances along the G axes – i.e., barycentric coordinates [7] (page 216). The origin of the texture space, i.e., the texture for which all block probabilities are equal, corresponds to $\vec{\sigma}_S = (1/G, 1/G, \ldots, 1/G)$, is at the centroid of each of these simplexes.

In sum (Table 1 of the main text), we began with the probabilities p of each of the G^4 ways of coloring a 2×2 block. Because these probabilities were drawn from a texture, there were consistency constraints among them that needed to be taken into account. These consistency constraints took on a simple form following Fourier transformation of the block probabilities. This transformation yielded the Fourier coordinates φ, which are complex numbers with $G(G-1)(G^2+G-1)$ free parameters. We then re-transformed the Fourier coordinates back into the domain of probabilities, leading to a grouping of these parameters into $G(G^2+G-1)$ vector quantities $\vec{\sigma}$, each of which are barycentric coordinates for a $G-1$-dimensional simplex. Table 1 of the main text also summarizes how these coordinates correspond to the system used in previous studies [1-6], in which $G=2$ and each of the 10 barycentric coordinate pairs reduce to scalars. This reduction corresponds to representing a 2-simplex, the line segment from $(1,0)$ to $(0,1)$, by a scalar that runs from -1 to 1.

1.3 Textures used in this study

The coordinates described above provide a formal description of the textures used in this study.

In Experiments 1 and 2, we used textures with three equally-spaced luminance levels (Figs. 1-4 of the main text, and Figs. S1 and S2). For $G=3$, the complete set of barycentric coordinates consist of $G(G^2+G-1)=33$ vectors: one first-order vector $\vec{\sigma}_{(1)}$; eight second-order vectors $\vec{\sigma}_{(1\ \ s)}$, $\vec{\sigma}_{\begin{pmatrix}1\\ s\end{pmatrix}}$, $\vec{\sigma}_{\begin{pmatrix}1 & \\ & s\end{pmatrix}}$, and $\vec{\sigma}_{\begin{pmatrix} & 1\\ s & \end{pmatrix}}$ for $s \in \{1,2\}$; 16 third-order vectors $\vec{\sigma}_{\begin{pmatrix}1 & s\\ s' & \end{pmatrix}}$ and its analogs rotated by 90, 180, or 270 deg in space, for $s, s' \in \{1,2\}$, and eight fourth-order vectors $\vec{\sigma}_{\begin{pmatrix}1 & s\\ s' & s''\end{pmatrix}}$ for $s, s', s'' \in \{1,2\}$.

In Experiment 1 we surveyed sensitivity to textures in which one of these vectors (i.e., one barycentric coordinate) was allowed to vary, and the rest were held at the origin. We then measured sensitivity for first-order vector $\vec{\sigma}_{(1)}$ (24 directions); the second-order vectors $\vec{\sigma}_{\begin{pmatrix}1\\ s\end{pmatrix}}$ and $\vec{\sigma}_{\begin{pmatrix}1 & \\ & s\end{pmatrix}}$ (12 directions each); the third-order vectors $\vec{\sigma}_{\begin{pmatrix}1 & 1\\ 1 & \end{pmatrix}}$, $\vec{\sigma}_{\begin{pmatrix}1 & 1\\ 2 & \end{pmatrix}}$, and $\vec{\sigma}_{\begin{pmatrix}1 & 2\\ 2 & \end{pmatrix}}$ (3 directions each), and the fourth-order vectors $\vec{\sigma}_{\begin{pmatrix}1 & 1\\ 1 & 1\end{pmatrix}}$. $\vec{\sigma}_{\begin{pmatrix}1 & 1\\ 1 & 2\end{pmatrix}}$, $\vec{\sigma}_{\begin{pmatrix}1 & 1\\ 2 & 2\end{pmatrix}}$, and $\vec{\sigma}_{\begin{pmatrix}1 & 2\\ 2 & 1\end{pmatrix}}$ (3 directions each). Each of the 33 vectors in the complete set for $G=3$ is either in this analyzed subset, or corresponds to an image statistic which, when rotated by 90, 180, or 270 deg or reflected in a cardinal axis, is in this set.

In Experiment 2, we studied textures specified by combinations of two second-order coordinates, for example, $\sigma_{(1\ \ 2),0}$ and $\sigma_{\begin{pmatrix}1\\ 1\end{pmatrix},2}$ (Fig. 4 of the main text). 22 such combinations were studied (Table S1), fully sampling the possible combinations of cardinal second-order correlations up to rotational and mirror symmetry.

The textures used in Experiment 3 had 3, 4, 5, 7, and 11 gray levels. Here, second-order correlations were chosen to create gradients (Fig. 5A of the main text) or streaks (Fig. 5B of the main text). In terms of the above parameterization, the gradients are specified by $\sigma_{(1\ \ G-1),1}$ (increasing luminance to left), $\sigma_{(1\ \ G-1),G-1}$ (increasing luminance to right), $\sigma_{\begin{pmatrix}1\\G-1\end{pmatrix},1}$ (increasing luminance up), $\sigma_{\begin{pmatrix}1\\G-1\end{pmatrix},G-1}$ (increasing luminance down). Streaks are specified by $\sigma_{(1\ \ G-1),0}$ (horizontal streaks), and $\sigma_{\begin{pmatrix}1\\G-1\end{pmatrix},0}$ (vertical streaks).

1.4 Texture synthesis

Most textures can be synthesized by the Markov method detailed in [1], which enables creation of textures specified by a single nonzero barycentric coordinate, or a pair of barycentric coordinates that correspond to correlations in the same spatial direction. This includes all of the stimuli for Experiments 1 and 3, and Group I (Table S1) of Experiment 2.

For the remaining textures, in which second-order correlations were present in two directions, a new construction-- "falling sticks" – is needed in some cases. This construction is described in [8] and summarized here. As a first step, a library of one-dimensional strips is created in each of the directions. For example, in the case of a Group III texture, horizontal strips correlated according to $\vec{\sigma}_{(1\ \ 1)}$, and vertical strips correlated according to $\vec{\sigma}_{\begin{pmatrix}1\\2\end{pmatrix}}$. Then, these strips are dropped at random onto the plane, with each newly-dropped strip covering up any strips that overlaps, until the entire lattice is covered. In a 1×2 region in which the final strip is horizontal, the correlation corresponding to $\vec{\sigma}_{(1\ \ 1)}$ is preserved. Alternatively, if one or two vertical strips landed on this region after the last horizontal strip, the colorings of the 1×2 checks are independent. Thus, the 1×2 correlations in the library of horizontal strips are diluted. The dilution factor is $1/3$ -- the probability that the last strip that landed on the 1×2 region is horizontal. Similar reasoning applies to the vertical correlations. Thus, provided that the desired correlations in the final texture are $\leq 1/3$, they can be achieved by judicious choice of the correlations in the original library of strips. First- and third-order correlations in the final texture are zero because they were absent in the original strips, and fourth-order correlations are present but small.

Note that the texture constructions described here are distinguished from those of [9] in that they take two-dimensional correlations into account, and are distinguished from those of [10]and [11] in that they have maximum-entropy guarantees.

2. Experimental Details

This section provides details of how texture domains were sampled in Experiments 1 and 2.

In Experiment 1, stimuli were defined by equally-spaced points lying along 12 rays in triangular domains corresponding to a genus of texture statistics (see Table 1 of the main text). Each ray began at the origin of the domain (the random texture) and extended either towards a vertex, or to points that were equally spaced along the edges of the domain (Fig. S1A). These sample points were used for the third- and fourth-order statistics. For second-order statistics, pilot studies showed that the textures at the vertices of the domain yielded ceiling performance, so the sample points along these rays were brought closer to the origin by a factor of 2/3 (Fig. S1B). For the same reason, distances along all rays were further shortened by a factor of 1/2 for the first-order statistics (Fig. S1C), and in this case, an additional set of 12 rays were interleaved to better delineate the threshold behavior.

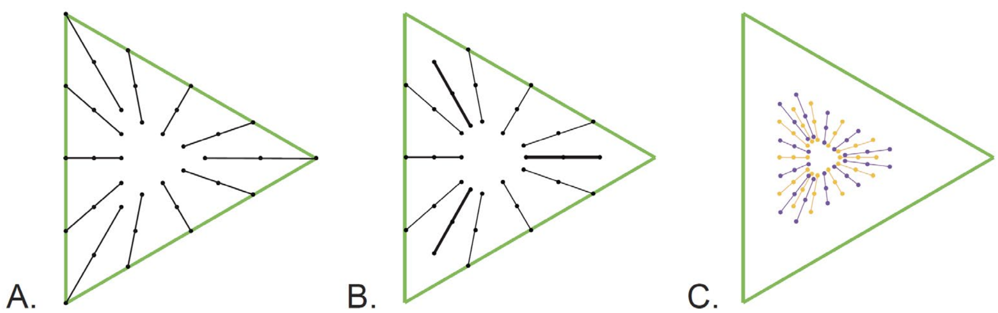

Fig. S1. Stimulus parameters used in Experiment 1. Each dot's position indicates the coordinates of a stimulus within a texture domain. A. For third- and fourth-order statistics, stimulus parameters were positioned along 12 rays (indicated by the black lines), each beginning at the origin of the domain and ending at the domain's boundary. B. For second-order statistics, distances from the origin along the rays directed towards the vertices (thicker lines) are reduced by a factor of 2/3 compared to Panel A. C. For first-order statistics, distances along all rays are further reduced by a factor of 1/2 compared to Panel B, and 12 additional rays are interleaved. The two sets of 12 rays, shown in separate colors, were tested in separate sessions.

In Experiment 2, stimuli were organized into four groups, as detailed in Table S1. Group I examined interactions between different statistics with the same family ($\vec{\sigma}_{(1\ \ 1)}$ and $\vec{\sigma}_{(1\ \ 2)}$, as in Fig. 4A,B of the main text); the other groups probed interactions between statistics from different families, describing correlations in orthogonal directions, $\vec{\sigma}_{(1\ \ s)}$ and $\vec{\sigma}_{\binom{1}{s'}}$: with $(s,s')=(1,1)$ in group II, $(s,s')=(1,2)$ in group III, and $(s,s')=(2,2)$ in group IV (the latter shown in Fig. 4C,D of the main text). All 22 domains (i.e., all 22 pairs of statistics) were sampled along rays in 12 equally-spaced directions, with three equally-spaced points along each ray. The position of the furthest points along the rays were determined by pilot studies, to ensure that they would be effective for measuring thresholds. These considerations resulted in the sampling strategies are shown in Fig. S2.

Table S1. Experiment 2 Design Details

group	second-order statistics			sampling
I	genus	$\vec{\sigma}_{(1\ \ 1)}$	$\vec{\sigma}_{(1\ \ 2)}$	
	species (vertex)	(1,0,0)	(1,0,0)	A
		(1,0,0)	(0,1,0)	A
		(0,1,0)	(1,0,0)	A
		(0,1,0)	(0,1,0)	A
		(0,0,1)	(1,0,0)	A
		(0,0,1)	(0,1,0)	A
II	genus	$\vec{\sigma}_{(1\ \ 1)}$	$\vec{\sigma}_{\left(\begin{smallmatrix}1\\1\end{smallmatrix}\right)}$	
	species (vertex)	(1,0,0)	(1,0,0)	B
		(0,1,0)	(0,1,0)	B
		(0,0,1)	(0,0,1)	B
		(1,0,0)	(0,1,0)	C
		(0,1,0)	(0,0,1)	C
		(0,0,1)	(1,0,0)	C
III	genus	$\vec{\sigma}_{(1\ \ 1)}$	$\vec{\sigma}_{\left(\begin{smallmatrix}1\\2\end{smallmatrix}\right)}$	
	species (vertex)	(1,0,0)	(1,0,0)	B
		(1,0,0)	(0,1,0)	C
		(0,1,0)	(1,0,0)	B
		(0,1,0)	(0,1,0)	C
		(0,0,1)	(1,0,0)	B
		(0,0,1)	(0,1,0)	C
IV	genus	$\vec{\sigma}_{(1\ \ 2)}$	$\vec{\sigma}_{\left(\begin{smallmatrix}1\\2\end{smallmatrix}\right)}$	
	species (vertex)	(1,0,0)	(1,0,0)	B
		(1,0,0)	(0,1,0)	B
		(0,1,0)	(1,0,0)	B
		(0,1,0)	(0,1,0)	B

Experiment 2 details. Each experimental group examines combinations of second-order statistics drawn from two genera, each corresponding to a triangular domain (as in Fig. 2 of the main text). Within each group, individual experiments differ according to the axes along which the statistics are varied. This axis -- the species -- is specified by a vertex of the triangular domain. The rightmost column indicates the design for sampling the domain generated by this combination of statistics, as illustrated in Fig. S2.

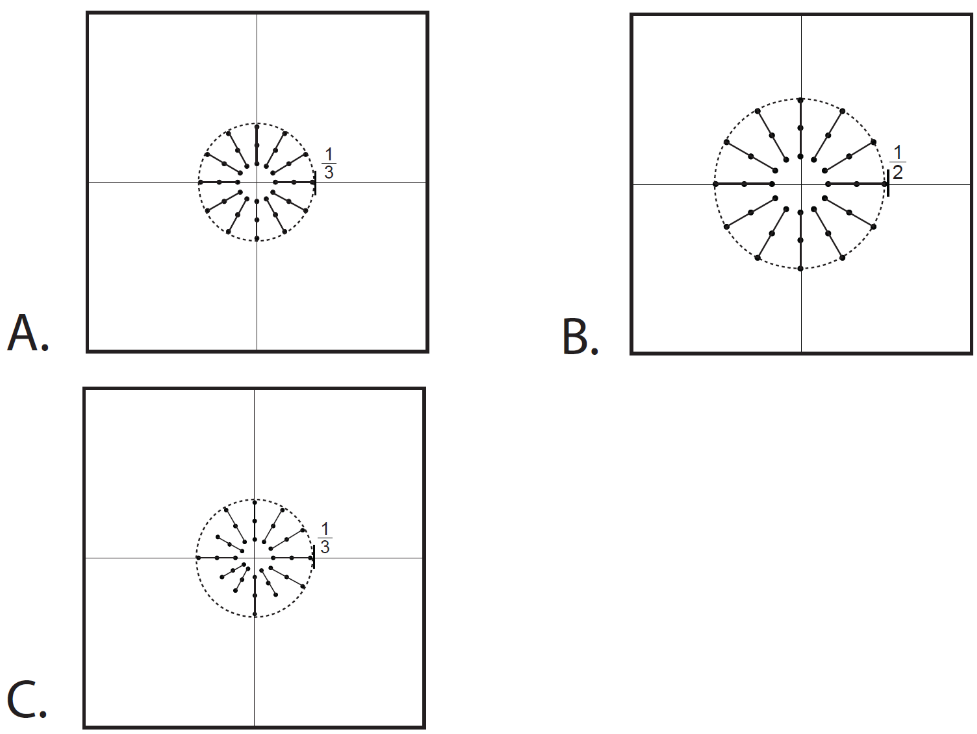

Fig. S2. Stimulus parameters used in Experiment 2. As in Fig. S1, each dot's position indicates the coordinates of a stimulus within a texture domain. The three sampling strategies (A, B, and C) correspond to the three designs indicated in Table S1. Each of these sampling strategies consist of 12 equally-spaced rays, with equidistant points along the rays chosen based on pilot studies. In A, the furthest points lie at a distance $1/3$ from the origin; in B, they lie at a distance $1/2$, and in C, they are $1/3$ on-axis and vary from $2/9$ to $1/3$ off-axis.

3. Specification of the model's quadratic form

Here we detail the calculations that specify the proposed model's quadratic form J, by requiring that the model's predictions for discrimination of black-and-white textures are consistent with previous experimental studies [3]. Ensuring that this is the case means that for any pair of black-and-white textures characterized by image statistics $\vec{y}$ and $\vec{y}'$, applying eq. (17) of the main text to their internal representations (i.e., the proposed model) must yield the same result as applying eq. (16) of the main text to $\vec{y}$ and $\vec{y}'$ (the empirical findings of [3]).

To work out the consequences of this requirement, we construct the binary block probabilities corresponding to $\vec{y}$ and $\vec{y}'$, then we apply eq. (15) of the main text to determine the image statistics of their internal representations, so that eq. (17) of the main text can be applied. Just as the image statistics are linear functions of the block probabilities via Y (eq. 14 of the main text), the block probabilities are linear functions of the image statistics, other than an offset corresponding to the block probabilities of the random texture. That is,

$$\vec{p}-\vec{p}'=(\vec{p}_{rand}+P\vec{y})-(\vec{p}_{rand}+P\vec{y}')=P(\vec{y}-\vec{y}') \tag{S20}$$

where $\vec{p}$ and $\vec{p}'$ are the block probabilities corresponding to the image statistics $\vec{y}$ and $\vec{y}'$, and $\vec{p}_{rand}$ assigns a probability of $1/16$ to each of the 16 possible binary 2×2 neighborhoods. The linear transformation P is given in Table 1 of [1] and here in Table S5; it is determined by the definition of the image statistics (eq. (S2)) and is not a model parameter. With eq. (15) of the main text, this yields a linear relationship between the difference between the binary image statistics $\vec{y}$ and $\vec{y}'$, and the difference between their internal representations $\vec{y}^{[m]}-\vec{y}'^{[m]}$:

$$\vec{y}^{[m]}-\vec{y}'^{[m]}=YL_2^{[m]}(\vec{p}-\vec{p}')=YL_2^{[m]}P(\vec{y}-\vec{y}') . \tag{S21}$$

Thus, the discrimination signal specified by eq. (17) of the main text is

$$S=\sum_m w_m(\vec{y}-\vec{y}')^T P^T L_2^{[m]T} Y^T J Y L_2^{[m]} P(\vec{y}-\vec{y}') . \tag{S22}$$

Since eqs.(S22) and main text eq. (16) are quadratic forms in the difference vector $\vec{y}-\vec{y}'$ that are identical for all choices of this vector, it follows that the quadratic forms themselves are equal:

$$\sum_m w_m P^T L_2^{[m]T} Y^T J Y L_2^{[m]} P = Q . \tag{S23}$$

Finally, eq. (S23) is a linear relationship between the elements of J and the elements of Q, with all the other quantities already specified, either from the Silva-Chubb parameters (w_m and $L_2^{[m]}$), or the definition of the image statistics (Y and P). Solving the set of linear equations yields J, which is given in Table S3.

4. Supplemental Tables for Computational Model

Table S2. Silva-Chubb Mechanisms

Activation Functions $F_m(x_i)$				
	Mechanism (m)			
Gray level (x_i)	1	2	3	4
0/8	0.6110	-0.6110	0.8730	-0.5679
1/8	0.4387	-0.4387	-0.1276	0.0936
2/8	0.2447	-0.2447	-0.3204	0.4330
3/8	0.0287	-0.0287	-0.2902	0.4847
4/8	-0.1478	0.1478	-0.1728	0.2851
5/8	-0.2915	0.2915	-0.0454	-0.0624
6/8	-0.3424	0.3424	0.0326	-0.2674
7/8	-0.2964	0.2964	0.0365	-0.2510
8/8	-0.2482	0.2482	0.0181	-0.1631
Weights (w_m)				
	Mechanism (m)			
Subject	1	2	3	4
S1	3.6279	3.3101	2.1911	2.8306
S2	3.5763	3.3565	2.5370	2.3111
S3	3.8363	3.1354	1.8562	2.2364
Average	3.6801	3.2673	2.1948	2.4594

Silva and Chubb [12] modeled the discrimination of IID textures in terms of four mechanisms, whose characteristics are defined by the four activation functions F_m (see eq. (6) of the main text). Columns list the values of $F_m(x_i)$ at nine equally-spaced gray level values x_i from black (0) to white (1); weights of these mechanisms as determined in the three subjects in that study; and the average across subjects, which were the values w_m used in this study. Numerical values kindly provided by C. Chubb.

Table S3. Model Matrices

Q: measured sensitivity to black-and-white textures										
	$y_1(\gamma)$	$y_2(\beta_{-})$	$y_3(\beta_{\mid})$	$y_4(\beta_{\backslash})$	$y_5(\beta_{/})$	$y_6(\theta_{\lrcorner})$	$y_7(\theta_{\llcorner})$	$y_8(\theta_{\ulcorner})$	$y_9(\theta_{\urcorner})$	$y_{10}(\alpha)$
$y_1(\gamma)$	32.340	-1.478	-1.478	0.888	0.888	1.864	1.864	1.864	1.864	-0.142
$y_2(\beta_{-})$	-1.478	13.370	1.480	0.169	0.169	-0.453	-0.453	-0.453	-0.453	2.156
$y_3(\beta_{\mid})$	-1.478	1.480	13.370	0.169	0.169	-0.453	-0.453	-0.453	-0.453	2.156
$y_4(\beta_{\backslash})$	0.888	0.169	0.169	6.754	3.045	-0.690	-1.059	-0.690	-1.059	-0.352
$y_5(\beta_{/})$	0.888	0.169	0.169	3.045	6.754	-1.059	-0.690	-1.059	-0.690	-0.352
$y_6(\theta_{\lrcorner})$	1.864	-0.453	-0.453	-0.690	-1.059	1.579	0.949	0.482	0.949	-0.390
$y_7(\theta_{\llcorner})$	1.864	-0.453	-0.453	-1.059	-0.690	0.949	1.579	0.949	0.482	-0.390
$y_8(\theta_{\ulcorner})$	1.864	-0.453	-0.453	-0.690	-1.059	0.482	0.949	1.579	0.949	-0.390
$y_9(\theta_{\urcorner})$	1.864	-0.453	-0.453	-1.059	-0.690	0.949	0.482	0.949	1.579	-0.390
$y_{10}(\alpha)$	-0.142	2.156	2.156	-0.352	-0.352	-0.390	-0.390	-0.390	-0.390	2.255
J: inferred sensitivity to internal binary representations										
	$y_1(\gamma)$	$y_2(\beta_{-})$	$y_3(\beta_{\mid})$	$y_4(\beta_{\backslash})$	$y_5(\beta_{/})$	$y_6(\theta_{\lrcorner})$	$y_7(\theta_{\llcorner})$	$y_8(\theta_{\ulcorner})$	$y_9(\theta_{\urcorner})$	$y_{10}(\alpha)$
$y_1(\gamma)$	56.067	-65.606	-65.606	-44.687	-44.687	12.033	12.033	12.033	12.033	-33.253
$y_2(\beta_{-})$	-65.606	42.940	20.940	1.525	1.525	-31.215	-31.215	-31.215	-31.215	28.823
$y_3(\beta_{\mid})$	-65.606	20.940	42.940	1.525	1.525	-31.215	-31.215	-31.215	-31.215	28.823
$y_4(\beta_{\backslash})$	-44.687	1.525	1.525	8.098	3.358	2.824	6.655	2.824	6.655	3.343
$y_5(\beta_{/})$	-44.687	1.525	1.525	3.358	8.098	6.655	2.824	6.655	2.824	3.343
$y_6(\theta_{\lrcorner})$	12.033	-31.215	-31.215	2.824	6.655	18.287	13.416	9.799	13.416	-50.568
$y_7(\theta_{\llcorner})$	12.033	-31.215	-31.215	6.655	2.824	13.416	18.287	13.416	9.799	-50.568
$y_8(\theta_{\ulcorner})$	12.033	-31.215	-31.215	2.824	6.655	9.799	13.416	18.287	13.416	-50.568
$y_9(\theta_{\urcorner})$	12.033	-31.215	-31.215	6.655	2.824	13.416	9.799	13.416	18.287	-50.568
$y_{10}(\alpha)$	-33.253	28.823	28.823	3.343	3.343	-50.568	-50.568	-50.568	-50.568	72.427

The matrices used to model sensitivity to local correlations. The matrix Q defines the quadratic form that accounts for discrimination of black-and-white textures with nearest-neighbor correlations (eqs. (10) and (16) of the main text). Q is determined in [3], which provided the eigenvalues and eigenvectors (Fig. 5A and Supplementary Table 1 of that reference) in four subjects; here, we use the average of the corresponding matrices. The matrix J defines the quadratic form in the present model that acts on internal binary representations produced by each of the Silva-Chubb mechanisms (eq. (17) of the main text). J is determined from the Silva-Chubb mechanisms (Table S2) and from Q, as the solution to eq. (S23).

Table S4. Conversion of Block Probabilities to Local Image Statistics

	$\begin{pmatrix}0&0\\0&0\end{pmatrix}$	$\begin{pmatrix}1&0\\0&0\end{pmatrix}$	$\begin{pmatrix}0&1\\0&0\end{pmatrix}$	$\begin{pmatrix}1&1\\0&0\end{pmatrix}$	$\begin{pmatrix}0&0\\1&0\end{pmatrix}$	$\begin{pmatrix}1&0\\1&0\end{pmatrix}$	$\begin{pmatrix}0&1\\1&0\end{pmatrix}$	$\begin{pmatrix}1&1\\1&0\end{pmatrix}$	$\begin{pmatrix}0&0\\0&1\end{pmatrix}$	$\begin{pmatrix}1&0\\0&1\end{pmatrix}$	$\begin{pmatrix}0&1\\0&1\end{pmatrix}$	$\begin{pmatrix}1&1\\0&1\end{pmatrix}$	$\begin{pmatrix}0&0\\1&1\end{pmatrix}$	$\begin{pmatrix}1&0\\1&1\end{pmatrix}$	$\begin{pmatrix}0&1\\1&1\end{pmatrix}$	$\begin{pmatrix}1&1\\1&1\end{pmatrix}$
$y_1(\gamma)$	-1	-1/2	-1/2	0	-1/2	0	0	1/2	-1/2	0	0	1/2	0	1/2	1/2	1
$y_2(\beta_-)$	1	0	0	1	0	-1	-1	0	0	-1	-1	0	1	0	0	1
$y_3(\beta_\vert)$	1	0	0	-1	0	1	-1	0	0	-1	1	0	-1	0	0	1
$y_4(\beta_\backslash)$	1	-1	1	-1	1	-1	1	-1	-1	1	-1	1	-1	1	-1	1
$y_5(\beta_/)$	1	1	-1	-1	-1	-1	1	1	1	1	-1	-1	-1	-1	1	1
$y_6(\theta_\lrcorner)$	-1	-1	1	1	1	1	-1	-1	1	1	-1	-1	-1	-1	1	1
$y_7(\theta_\llcorner)$	-1	1	-1	1	1	-1	1	-1	1	-1	1	-1	-1	1	-1	1
$y_8(\theta_\ulcorner)$	-1	1	1	-1	1	-1	-1	1	-1	1	1	-1	1	-1	-1	1
$y_9(\theta_\urcorner)$	-1	1	1	-1	-1	1	1	-1	1	-1	-1	1	1	-1	-1	1
$y_{10}(\alpha)$	1	-1	-1	1	-1	1	1	-1	-1	1	1	-1	1	-1	-1	1

The matrix Y (eq (14) of the main text) that converts block probabilities to local image statistics. It is determined by the definitions of the image statistics. Elements of Y determines the weighting factor by which the probability of the 2×2 block at the top of each column contributes to the image statistic at the beginning of each row.

Table S5. Conversion of Local Image Statistics to Block Probabilities

	$y_1(\gamma)$	$y_2(\beta_{-})$	$y_3(\beta_{\mid})$	$y_4(\beta_{\backslash})$	$y_5(\beta_{/})$	$y_6(\theta_{\lrcorner})$	$y_7(\theta_{\llcorner})$	$y_8(\theta_{\ulcorner})$	$y_9(\theta_{\urcorner})$	$y_{10}(\alpha)$
$\begin{pmatrix} 0 & 0 \\ 0 & 0 \end{pmatrix}$	-4/16	2/16	2/16	1/16	1/16	-1/16	-1/16	-1/16	-1/16	1/16
$\begin{pmatrix} 1 & 0 \\ 0 & 0 \end{pmatrix}$	-2/16	0/16	0/16	-1/16	1/16	-1/16	1/16	1/16	1/16	-1/16
$\begin{pmatrix} 0 & 1 \\ 0 & 0 \end{pmatrix}$	-2/16	0/16	0/16	1/16	-1/16	1/16	-1/16	1/16	1/16	-1/16
$\begin{pmatrix} 1 & 1 \\ 0 & 0 \end{pmatrix}$	0/16	2/16	-2/16	-1/16	-1/16	1/16	1/16	-1/16	-1/16	1/16
$\begin{pmatrix} 0 & 0 \\ 1 & 0 \end{pmatrix}$	-2/16	0/16	0/16	1/16	-1/16	1/16	1/16	1/16	-1/16	-1/16
$\begin{pmatrix} 1 & 0 \\ 1 & 0 \end{pmatrix}$	0/16	-2/16	2/16	-1/16	-1/16	1/16	-1/16	-1/16	1/16	1/16
$\begin{pmatrix} 0 & 1 \\ 1 & 0 \end{pmatrix}$	0/16	-2/16	-2/16	1/16	1/16	-1/16	1/16	-1/16	1/16	1/16
$\begin{pmatrix} 1 & 1 \\ 1 & 0 \end{pmatrix}$	2/16	0/16	0/16	-1/16	1/16	-1/16	-1/16	1/16	-1/16	-1/16
$\begin{pmatrix} 0 & 0 \\ 0 & 1 \end{pmatrix}$	-2/16	0/16	0/16	-1/16	1/16	1/16	1/16	-1/16	1/16	-1/16
$\begin{pmatrix} 1 & 0 \\ 0 & 1 \end{pmatrix}$	0/16	-2/16	-2/16	1/16	1/16	1/16	-1/16	1/16	-1/16	1/16
$\begin{pmatrix} 0 & 1 \\ 0 & 1 \end{pmatrix}$	0/16	-2/16	2/16	-1/16	-1/16	-1/16	1/16	1/16	-1/16	1/16
$\begin{pmatrix} 1 & 1 \\ 0 & 1 \end{pmatrix}$	2/16	0/16	0/16	1/16	-1/16	-1/16	-1/16	-1/16	1/16	-1/16
$\begin{pmatrix} 0 & 0 \\ 1 & 1 \end{pmatrix}$	0/16	2/16	-2/16	-1/16	-1/16	-1/16	-1/16	1/16	1/16	1/16
$\begin{pmatrix} 1 & 0 \\ 1 & 1 \end{pmatrix}$	2/16	0/16	0/16	1/16	-1/16	-1/16	1/16	-1/16	-1/16	-1/16
$\begin{pmatrix} 0 & 1 \\ 1 & 1 \end{pmatrix}$	2/16	0/16	0/16	-1/16	1/16	1/16	-1/16	-1/16	-1/16	-1/16
$\begin{pmatrix} 1 & 1 \\ 1 & 1 \end{pmatrix}$	4/16	2/16	2/16	1/16	1/16	1/16	1/16	1/16	1/16	1/16

The matrix P (eq. (S20)) that converts local image statistics to block probabilities. The matrix is determined by the definitions of the image statistics. Elements of P determine the weighting factor by which the image statistic at the top of each column contributes to the probability of the 2×2 block at the beginning of each row. Note that $YP = I$, where Y is given by Table S4.

5. References

1. J. D. Victor, and M. M. Conte, "Local image statistics: maximum-entropy constructions and perceptual salience," J Opt Soc Am A Opt Image Sci Vis **29**, 1313-1345 (2012).
2. J. D. Victor, S. M. Rizvi, and M. M. Conte, "Two representations of a high-dimensional perceptual space," Vision Res **137**, 1-23 (2017).
3. J. D. Victor, D. J. Thengone, S. M. Rizvi, and M. M. Conte, "A perceptual space of local image statistics," Vision Res **117**, 117-135 (2015).
4. A. M. Hermundstad, J. J. Briguglio, M. M. Conte, J. D. Victor, V. Balasubramanian, and G. Tkacik, "Variance predicts salience in central sensory processing," eLife **3** (2014).
5. J. D. Victor, D. J. Thengone, and M. M. Conte, "Perception of second- and third-order orientation signals and their interactions," J Vis **13**, 21 (2013).
6. J. D. Victor, S. M. Rizvi, and M. M. Conte, "Image segmentation driven by elements of form," Vision Res (2019).
7. H. S. M. Coxeter, *Introduction to Geometry Second Edition* (John Wiley & Sns, 1969).
8. T. Tesileanu, M. M. Conte, J. J. Briguglio, A. M. Hermundstad, J. D. Victor, and V. Balasubramanian, "Efficient coding of natural scene statistics predicts discrimination thresholds for grayscale textures," eLife **9** (2020).
9. R. Yokoyama, and R. M. Haralick, "Texture pattern image generation by regular markov chain," Pattern Recognition **11**, 225-234 (1979).
10. J. Portilla, and E. P. Simoncelli, "A parametric texture model based on joint statistics of complex wavelet coefficients," International Journal of Computer Vision **40**, 49-71 (2000).
11. A. Darzi, I. Lang, A. Talikar, H. Averbuch-Elor, and S. Avidan, "Co-occurrence based texture synthesis," Computational Visual Media **8**, 289-302 (2021).
12. A. E. Silva, and C. Chubb, "The 3-dimensional, 4-channel model of human visual sensitivity to grayscale scrambles," Vision Res **101**, 94-107 (2014).